ORIGINAL ARTICLE
DOI: https://doi.org/10.18599/grs.2020.3.69-78 Russian Original 2020. Vol. 22. Is. 3. Pp. 69–78

Junction zone stability in coaxial wells of different diameters (on the example of the Khanty-Mansi Autonomous District oil field)

A.V. Seryakov[1], M.Yu. Podberezhny[2], O.B. Bocharov[1], M.A. Azamatov[3]*
[1]*Novosibirsk Technology Center, Baker Hughes, Novosibirsk, Russian Federation*
[2]*Gazpromneft-GEO, St. Petersburg, Russian Federation*
[3]*Salym Petroleum Development N.V., Moscow, Russian Federation*

Abstract. The paper considers borehole wall stability in a junction zone of coaxial wells where a borehole of bigger diameter connects with a smaller one. To determine the shapes and character of rock destruction, 3D poroelastic modeling of the stressed state of the rock around the coaxial junction with account for mudcake formation was performed. The geomechanical model considers the anisotropy of the medium's deformation properties that are characteristic for the coastal-marine reservoirs of Western Siberia. The rock failure is estimated based on the Mohr-Coulomb criterion with account for tensile destruction condition. The paper considers cases of vertical and inclined junctions of a well drilled at a depth of 2 km in sandstone productive pay with known poroelastic anisotropic properties. The stress and pore pressure analysis has been performed for a mud pressure drop range from 1 to 70 atm and coaxial junctions with different combinations of borehole diameters. The safe mud pressure window has been determined for vertical and inclined junctions. It has been found that the rock failure pattern for junction of bigger diameters is, in general, similar to that for smaller diameters with some insignificant differences in the destruction areas shapes. It has also been demonstrated that in vertical junctions, the bottom holes of smaller diameter are more stable to reduced drilling-mud pressure than the main boreholes, while in the inclined junction it is the main wellbore that is more stable to increased drilling-mud pressure than the bottom hole.

Keywords: 3D poroelastic modeling, coaxial junction, vertical and inclined well, anisotropy, rock failure, sandstone reservoir

Recommended citation: Seryakov A.V., Podberezhny M.Yu., Bocharov O.B., Azamatov M.A. (2020). Junction zone stability in coaxial wells of different diameters (on the example of the Khanty-Mansi Autonomous District oil field). *Georesursy = Georesources*, 22(3), pp. 69–78. DOI: https://doi.org/10.18599/grs.2020.3.69-78

Introduction

In prospecting drilling (especially with mobile drilling units) it is a common situation when one has to drill deeper for core sampling and logging, but the unit's capacity does not permit to do it using a bit of the same diameter. This problem is often solved by shifting to a smaller bit diameter to drill in the same hole, but this raises an issue of junction zone stability in such coaxial wells (Figure 1) because intensive bursting of rock chips from a borehole wall leads to their accumulation in the bottom hole.

During sequential core sampling pieces of rock can stick in the core barrel causing its locking that requires additional round-trips to resolve. Moreover, enlarging the bottom hole to match the main wellbore diameter after core sampling and logging are finalized requires the junction zone stability to be assessed.

The stability of different diameters boreholes junction is the relevant problem of core drilling operations at the

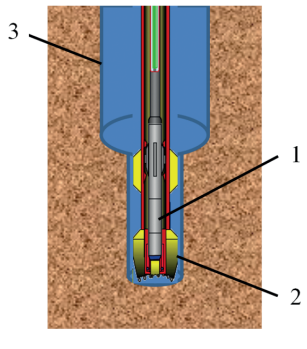

Fig. 1. Junction zone configuration after core extraction to the sampler barrel (1) in the case when core drilling bit (2) diameter is less than the one of the main borehole (3)

*Corresponding author: Alexandr V. Seryakov
E-mail: alexander.seryakov@bakerhughes.com

oilfields of Khanty-Mansi Autonomous District in Russia (KhMAD). In spite of its urgency the problem statement, description and solution approaches are not presented in the literature sources. It should be noted that there are the similar tasks of tube junction resistance to the inner pressure or external loading increasing (e.g. Grogulenko, 2017) that are solved with the help of the elastoplastic models in commercial computation packages. However such modeling doesn't take into account physical processes in porous rock near the wellbore junction zone at a kilometers depth.

Wellbore stability of the junction should be assessed with the help of the poroelastic modeling that includes non-uniform stress distribution, rock anisotropy, mudcake formation due to the mud filtration into the productive pay.

It should be pointed out that 2D approaches to the stress and pore pressure determination around wellbore (Cui et al., 1997; Liu et al., 2018) have the restricted application in the considered case since the stress distribution close to the junction plane will be essential three dimensional.

Assef Mohamad-Hussein and Julian Heiland (Mohamad-Hussein, Heiland, 2018) successfully performed poro-elasto-plastic modeling and analysis for the multilateral wellbore junction. The hardening porous material model and plastic surface based on the Mohr-Coulomb failure criteria are used in the 3D finite element computations.

We consider the simpler case of wellbore junction configuration and apply the vertical transversely isotropic poroelastic model with mudcake formation taken into account for effective stresses determination and rock failure estimation based on the Mohr-Coulomb criteria.

The modeling goal is the safe mud window determination for the vertical and inclined coaxial wellbore junction.

Rock characteristics

The modeling was performed for the rocks of the Neocomian age (the Akh Formation productive pays) that belong to the fields of the Surgut Dome and are characterized with the coastal-marine sedimentation conditions. The reservoirs of the formation are aleurolitic sandstones of 13–20% porosity and 10–100 mD permeability (Figure 2) overlaid by argillite-like clays. Cross-dipole acoustic and electromagnetic measurements and core analysis results indicate the anisotropic properties of these rocks (anisotropy coefficient 1–10%). As it was demonstrated in (Seryakov et al., 2018), vertical and inclined wells stability analysis has to be performed considering the anisotropy of rock's poroelastic properties.

Problem statement

Sandstone productive pay at a fixed depth of 2400 m is considered. At such a depth sandstone's petrophysical properties are anisotropic and experimental data of core deformation tests have the better fit with transversal isotropic poroelastic model.

In the reservoir, we model the junction of vertical and inclined sections of an open well, where a main borehole of bigger diameter D_1 meets a bottom hole of smaller diameter D_2 (Figure 3). The inclined well is characterized by angle ψ (60°) to the vertical axis and azimuthal angle β (25°) to the direction of the maximum horizontal stress. The model has been considered for two characteristic diameter ratios: I. D_1 = 220 mm, D_2 = 160 mm; II. D_1 = 160 mm, D_2 = 120 mm.

It is assumed that both parts of a well in the junction zone experience similar drilling-mud pressure P_b that exceeds reservoir pressure P_0 by value dP. The previous studies interpreting electromagnetic measurements from the oilfields of KhMAD have demonstrated that a weakly-permeable mud cake forms on borehole walls while drilling. The laboratory studies such as that of (Podberezhny et al., 2017) determine this layer's permeability to be 0.001 mD. In our modeling, we applied the mudcake growth model presented in (Podberezhny et al., 2017).

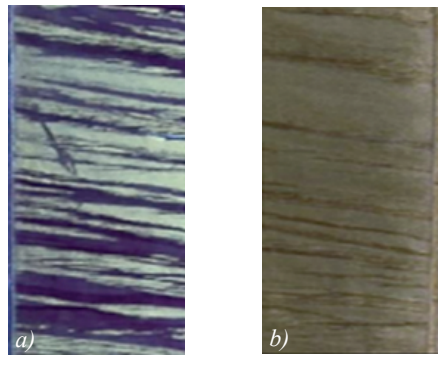

Fig. 2. Aleurolitic sandstone with lenticular bedding; a) – in ultraviolet light; b) – in daylight

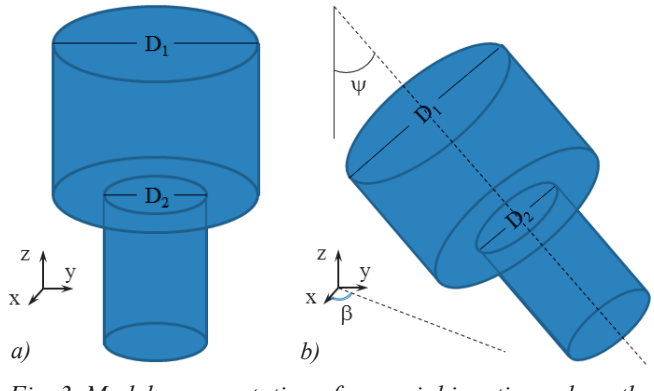

Fig. 3. Model representation of a coaxial junction, where the main borehole has a bigger diameter than the bottom hole: a) – vertical well, b) – inclined well

Poroelastic model

To determine the stress-strain state of the rock surrounding the junction zone, a vertical transversely isotropic poroelastic model was used. Its detailed description can be found in (Cheng, 1997) with the simplifications for poroelastic coefficients presented in (Seryakov et al., 2018). The model is characterized by the homogeneous properties in the plane perpendicular to the symmetry axis Z, which is commonly selected to match rock stratification direction in a geological medium. To describe the deformations of elastic rock matrix one has to set 5 constants that include two Young's modula E, E'; two Poison's ratios ν, ν'; and one shear module G' (Figure 4). The modeling was performed for a fixed depth and the following constant values: $E' = 12$ *GPa*, $E = 13$ *GPa*, $\nu' = 0.16$, $\nu = 0.17$, $G' = 5.17$ *GPa*.

The medium's permeability was considered equal to 50 mD.

According to geophysics data offered by the operating companies, the Biot-Willis coefficient for the coastal-marine sedimentation reservoirs of KhMAD is $\alpha = 0.95$. The additional poroelastic constants were derived from the main dependencies of the linear poroelastic theory that includes triaxial matrix compression coefficient, fluid compression and porosity coefficients. More details on the constants and their formulas can be found in Bocharov (Bocharov, Seryakov, 2016). Considering that the porosity $\phi = 0.23$, unjacketed bulk compressibility modulus $K'_S = 36$ GPa, fluid compressibility $K_f = 3$ GPa, we obtained the Skempton coefficient B = 0.5 and the Biot module M = 13.38 GPa.

The initial stress state around well was derived from the geophysical data on regional stresses distribution corrected for reservoir microfracturing tests, while the porous pressure was estimated based on logging interpretation results. At the fixed depth, the stresses had the following values: $\sigma_v = \sigma_{zz} = 54$ MPa, $\sigma_{hmax} = \sigma_{xx} = 36$ MPa, $\sigma_{hmin} = \sigma_{yy} = 34$ MPa. The reservoir's porous pressure was $P_0 = 25$ MPa. The ratio of vertical and horizontal stresses indicated the field developed in the normal faulting regime (Zoback, 2010).

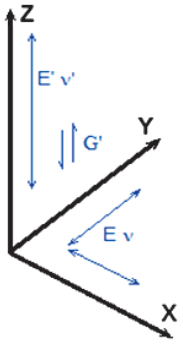

Fig. 4. Transversal-isotropic modules in a continuum medium

When modeling the junction's stressed state under pressure, the growing mud cake was taken into account. The considered mudcake properties included mudcake permeability $k_c = 0.001$ mD, porosity $\phi_c = 0.3$, and suspended particle concentration in the drilling mud (6%). Except for the mud cake, we also accounted for colmatation zone assuming the reducing formation permeability $k_d = 5$ mD (= 0.1k) within 1cm from the well's contour.

The application of a transversely isotropic model to rock deformation description also implies the rock failure criterion in which the strength of the material depends on the angle of inclination of considering plane to the bedding (Ashikhmin, 2018; Geniev, 1993). However due to the lack of experimental data on in-situ rock strength characteristics in different directions, the isotropic Coulomb-Mohr criterion was applied at the first stage of the study:

$$\sigma_1 - \sigma_3 ctg\psi = C_0, \quad (1)$$

where σ_1, σ_3 denote the main effective stresses; $ctg\psi = (1+\sin\varphi)/(1-\sin\varphi)$, φ is the inner friction angle, C_0 is the unconfined compressive strength. Analyzing the rock damage, we considered the equivalent stress function $\sigma_e = \sigma_1 - \sigma_3 ctg\psi$ that is convenient for visualization and comparison against C_0. The sandstone's strength properties at the given depth were taken from a laboratory core compression tests and equal to $\varphi = 30°$, $C_0 = 17$ MPa. The critical tensile stress σ_T for the sandstone was assigned equal to 1 MPa. The destruction type was determined in relation to the ratio of the main stresses and position relative to the plasticity curve (Fadeev, 1987) determined from (1) and the breaking condition

$$\sigma_1 < -\sigma_T, \quad (2)$$

where we adhered to the statement that tension stresses were negative. Therefore if the medium's stressed state was in the plasticity range, either breakouts or hydrofracturing conditions could be realized in the rock.

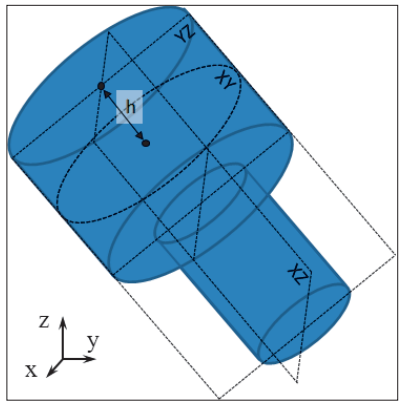

Fig. 5. Plane sections to visualize rock failure parameters for a 3D model

The computations were performed using the Geofluid package, whose FEM-based iteration algorithm has been described in particular in (Rudyak et al., 2013).

Results of modeling

Modeling of the two types of junctions, both vertical and inclined ones, started with a basic case, for which the value of pressure drop on borehole wall was 40 atm and corresponded to the "standard" overpressure while drilling in the hydrocarbon fields of KhMAD. For every other computation that follow, the pressure drop was either increased or reduced by 5–10 atm within a range from 1 to 70 atm.

The destruction area and equivalent stress field visualization in 3D domain was performed along the XY, YZ and XZ plane sections. For the vertical junction, these sections matched the reference planes, while for the inclined one were turned to match the well's angle (Figure 5).

Sections XY were characterized by the distance h from the upper section perpendicular to the well's axis to the studied plane. The distances from the top to the bottom perpendicular sections of the modeled domain was 2 m, and the transition area (from the main hole's diameter to that of the bottom hole) was h = 1.0 m.

Vertical junction

In the 220/160 mm junction, the standard pressure drop forms a concentric local-depth domain of shear fracturing situated in the main hole next to where the two diameters meet (Figure 6). This figure and the following depict the isolines of the parameter σ_e. In the figures, the blue digits mark the values of equivalent stresses in MPa and the areas of shear rock failure are filled with red color.

Considering the fact that the destruction is local and that its length along the z-axis is about 5 cm, the junction can be described as conditionally stable.

At the same pressure drop, modeling of a 160/120 mm junction demonstrates a similar character of destruction but with changed equivalent-stress distribution if compared to the previous case (Figure 7).

In fact, redistribution of formation stresses occur at the level of h = 1 m (right at the junction) and the differences

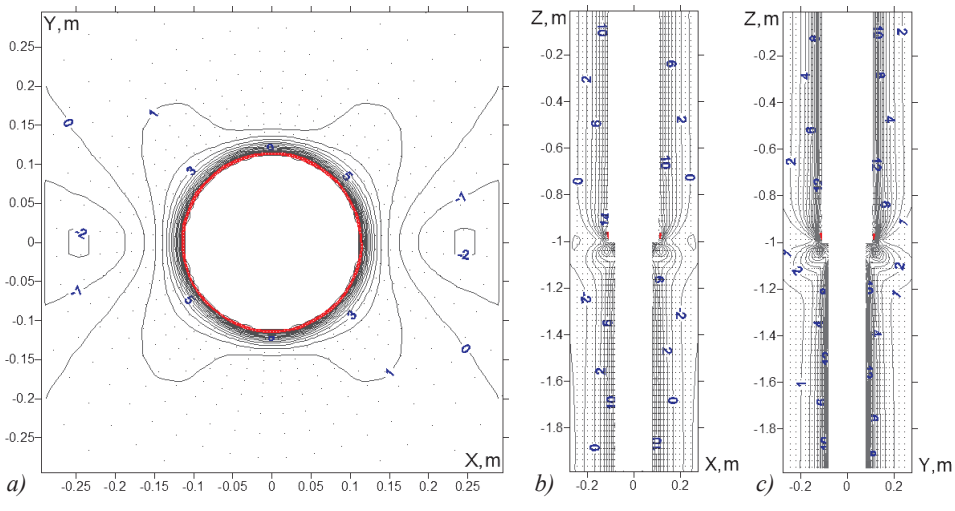

Fig. 6. Destruction areas in a vertical 220/160 mm junction at dP = 40 atm: the XY (a, h = 0.99 m), XZ (b), YZ (c) planes

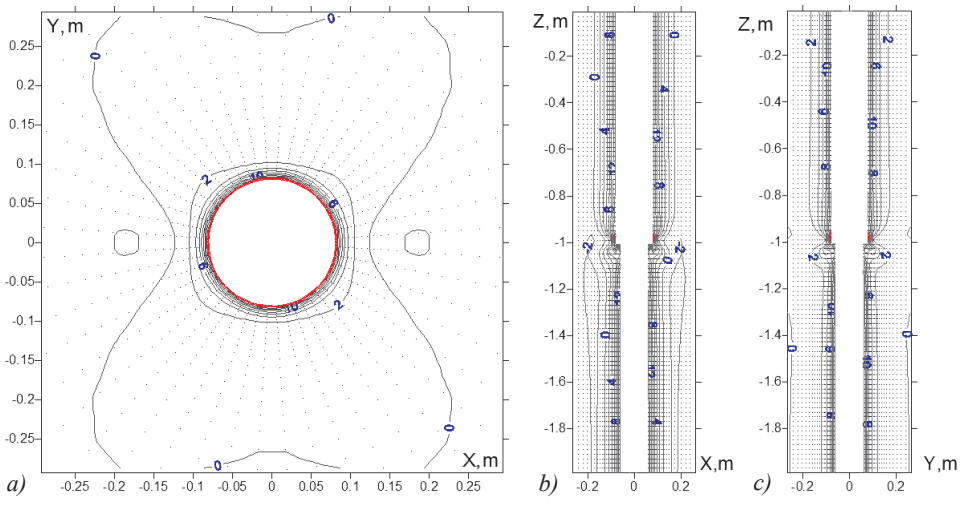

Fig. 7. Destruction areas in a vertical 160/120 mm junction at dP = 40 atm: the XY (a, h = 0.99 m), XZ (b), YZ (c) sections

in the stress value $\sigma_в$ between the two junctions may exceed 50%. Moreover, for the 160/120 mm junction the stress gradients increase and the stresses change faster than those of 220/160 mm junction. However, when it comes to the midsections of the wells (h = 0.5 m, h = 1.5 m), $\sigma_в$ behaves much smoother, so the differences between the cases do not exceed 12%.

If the pressure drop decreases to 35 atm, the rock failure area around the main borehole starts to spread downward into the formation forming the semiring depicted in Figure 8.

The formation around the 160/120 mm junction experiences similar changes but the rock failure area forms a closed ring below the main diameter (Figure 9).

Thus, one should expect concentric pieces of rock to split off from the wall and fall down into a borehole of the smaller diameter while drilling an uncased well.

Further decrease in the pressure drop results in the widening of the shear fracturing area that spreads deeper into the formation and propagating along the walls of wellbore both bigger and smaller diameters (Figure 10). In other words, drilling at a pressure drop of below 40 atm makes the junction's walls unstable.

In the opposite scenario, when the pressure drop increases to 55 atm, the rock failure area in the main borehole reduces, breaking the ring of fractured rock as shown in Figure 11. It is noteworthy that in the 160/120 mm junction, the width of the fracturing area also reduces (Figure 11 c).

Further dP increase up to 60 atm leads to complete elimination of the fracturing areas in the vertical junctions. It is noteworthy that even at 70 atm, dP increase does not provoke hydrofracturing.

Inclined junctions

In an inclined 220/160 mm junction, the standard dP of 40 atm induces breakouts of both main and bottom holes, which can be seen from the XY sections at heights of h = 0.99 m (a) and h = 1.01 m (b) on Figure 12. Moreover, the junction's shoulder contains a

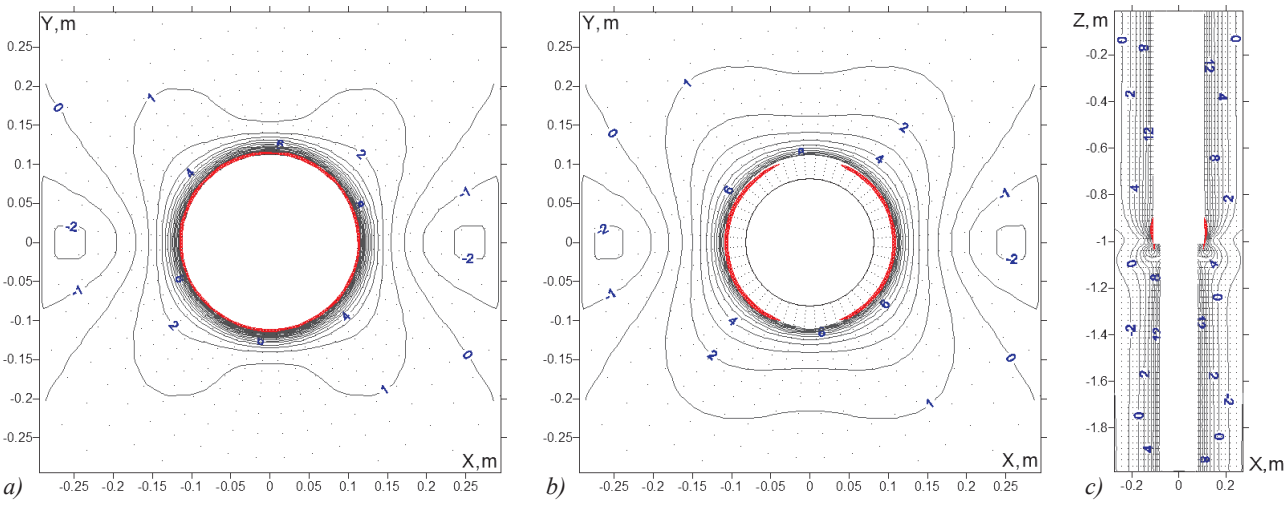

Fig. 8. Rock failure propagation in a vertical 220/160 mm junction at reduced dP (35 atm). The XY section is shown for h = 0.99 m (a) and h = 1.01 m (b). The vertical extent of the fracturing area is shown in the XZ section (c)

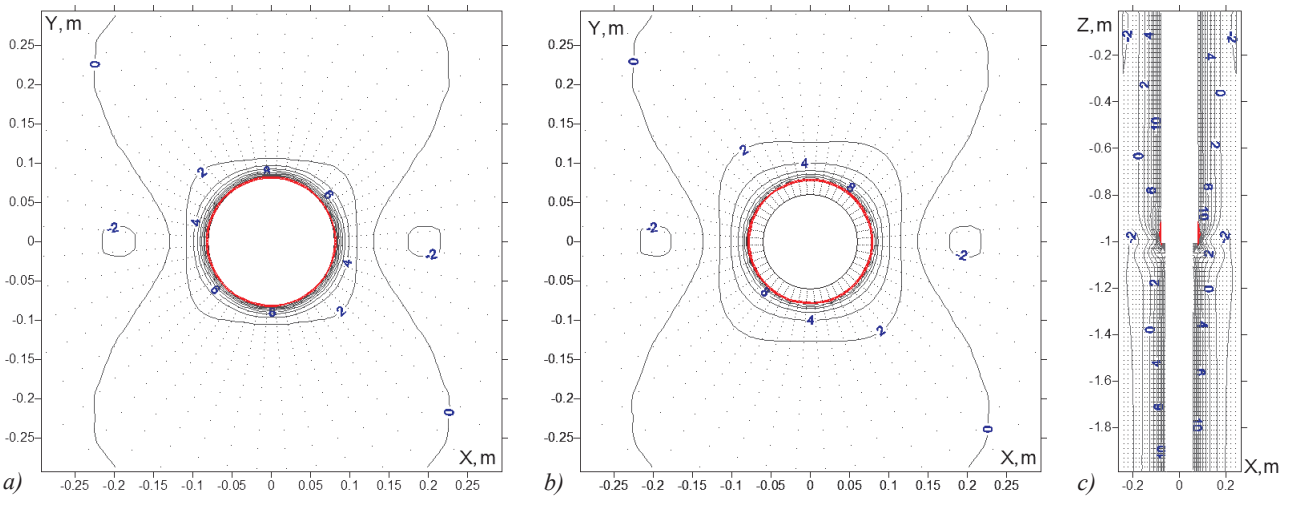

Fig. 9. Rock failure propagation in a vertical 160/120 mm junction at reduced dP (35 atm). The XY section is shown for h = 0.99 m (a) and h = 1.01 m (b). The vertical extent of the destructed area is shown in the XZ section (c)

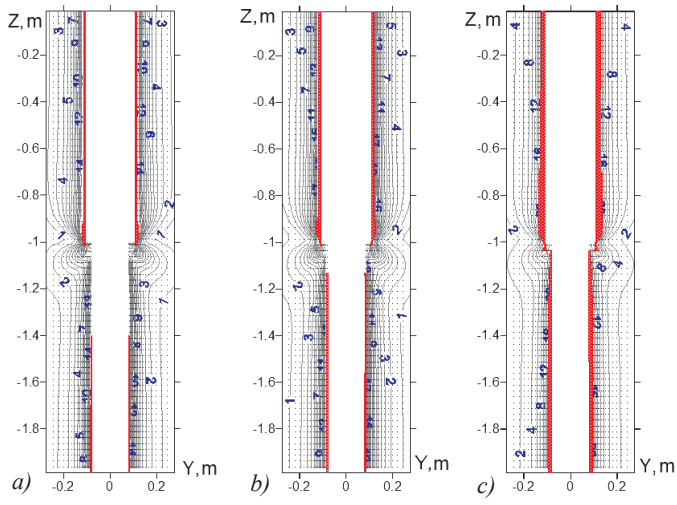

Fig. 10. Increasing of the breakouts area in the XZ section of a 220/160 mm junction at the pressure drop reduced to 30 atm (a), to 20 atm (b) and to 1 atm (c)

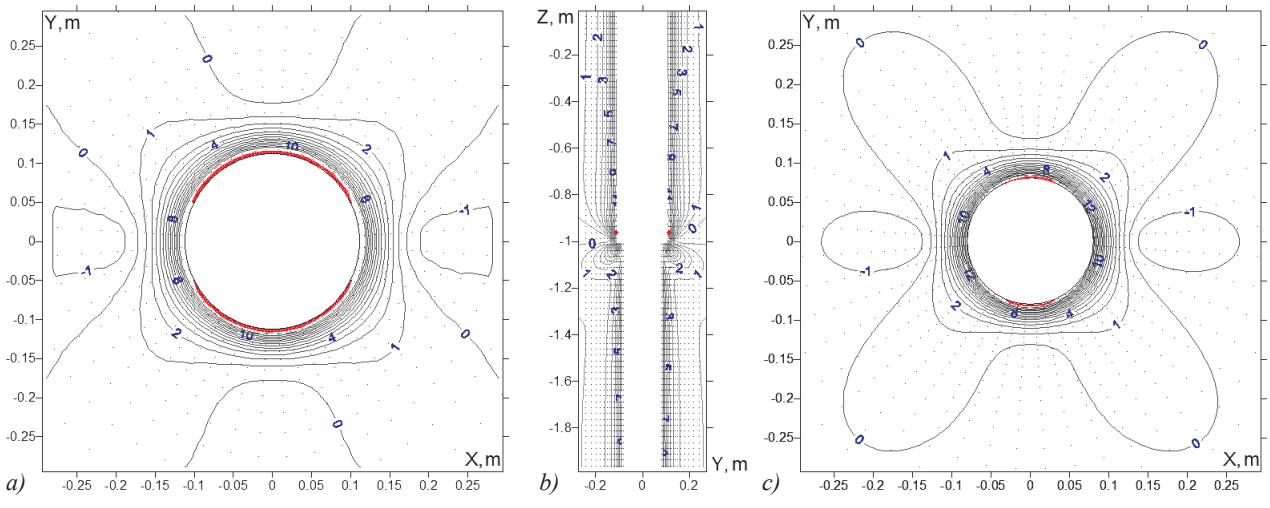

Fig. 11. Rock failure at increased pressure drop (dP = 55 atm) in the XY (h = 0.97 m) and YZ section of a 220/160 mm junction and the XY (h = 0.97 m) section of a 160/120 mm junction (c)

hydrofracture marked in yellow (Figure 12, b, d). The breakouts area extension can be traced from the XZ section since the shear failures are mainly directed along the direction of minimum horizontal stress (Figure 12, c). At the same time, the YZ section oriented mainly in the direction of maximum horizontal stress gives a good image of the hydrofracture (Figure 12, d). For its better visualization, the YZ section image has been enlarged.

Considering the fact that the angular size of the shear fracturing exceeds 90° (Figure 12, a), such a junction should be regarded as unstable (Zoback, 2010).

Observing analogous sections for the 160/120 mm juncture, we can see the destruction areas of a similar character and type appeared in sandstone (Figure 13). Since the angular size of the fracturing area still exceeds 90°, it is regarded as unstable as well. Analogous to the case of 220/160 mm diameters ratio, a hydrofracture formed within the juncture's shoulder (Figure 13, b, d)

Let's analyze how the pressure drop decreasing will affect the destruction zones. It should be noted that expected hydrofrac elimination does not happen when reducing dP. There is always at least one damaged cell within the juncture's shoulder and it is so for both for 220/160 mm and 160/120 mm cases. On the other hand, the reduced dP leads to increasing the breakouts area, since the compressing stresses around the holes increase. The way the shapes of destructed areas change can be seen in Figure 14 demonstrating simulation results for the 220/160 mm juncture at dP = 20 atm. In this case, the shear failure area increases both along the well's contour and in the radial direction.

At reduced pressure drop, the inclined 160/120 mm junction demonstrates the behavior similar to the one described for the 220/160 mm and for that reason is omitted.

Further reduction of dP down to 1 atm results in shear failures almost close around the well, in other words, the walls collapse around the juncture.

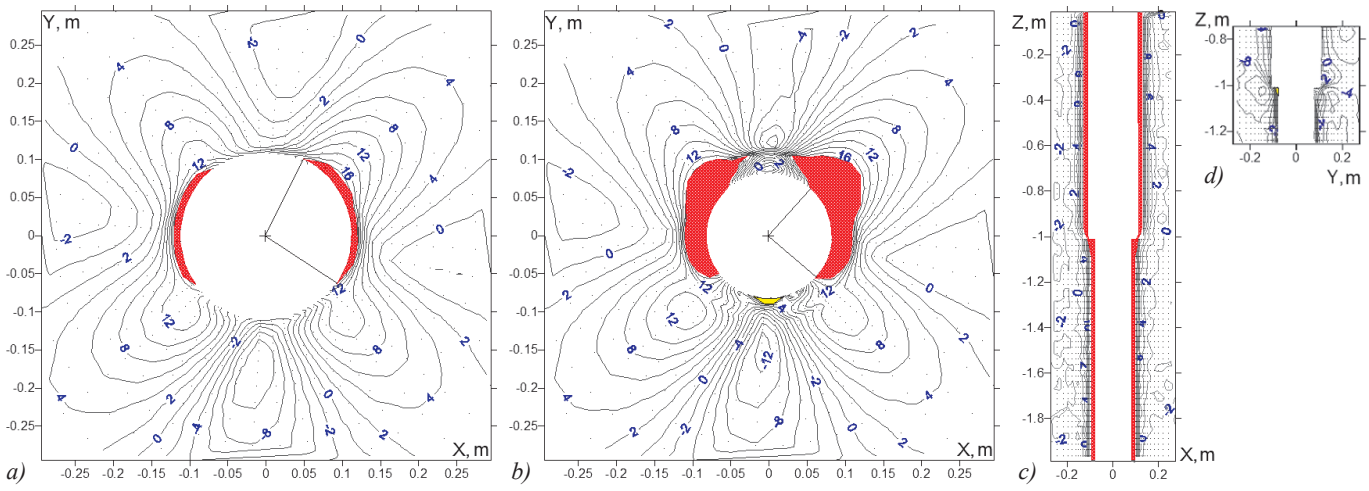

Fig. 12. Destruction areas in an inclined 220/160 mm junction at dP = 40 atm. The XY section is related to h = 0.99 m (a) and h = 1.01 m (b). Breakouts are marked in red in the XZ section (c). A hydrofracture is marked in yellow in the YZ section (d).

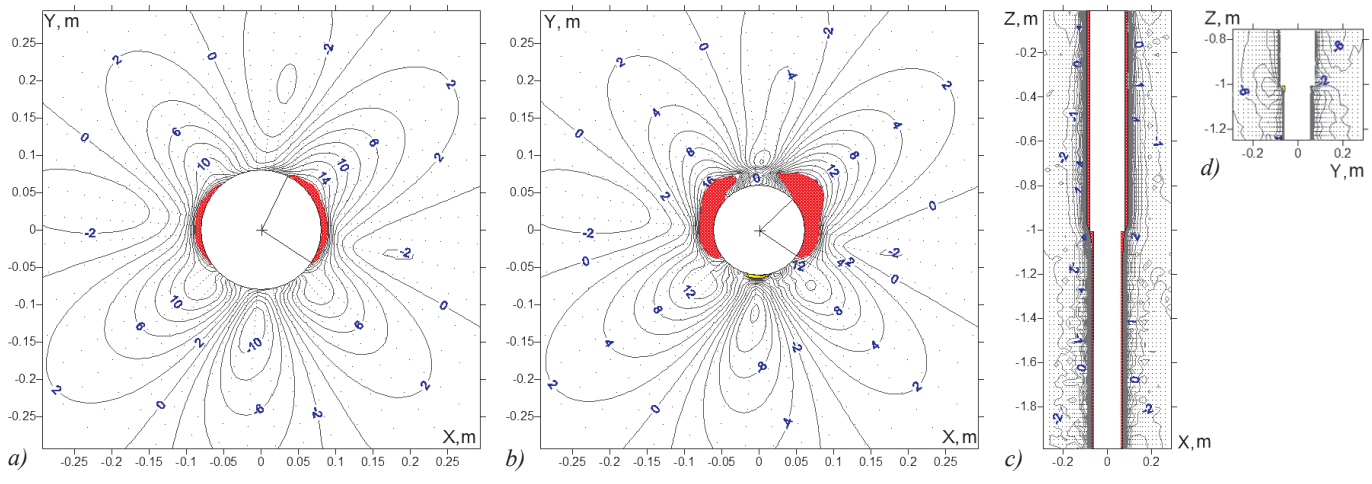

Fig. 13. Sandstone failure around an inclined 160/120 mm juncture at dP = 40 atm. The XY section is related to h = 0.99 m (a) and h = 1.01 m (b). The XZ and YZ sections can be seen in (c) and (d), respectively.

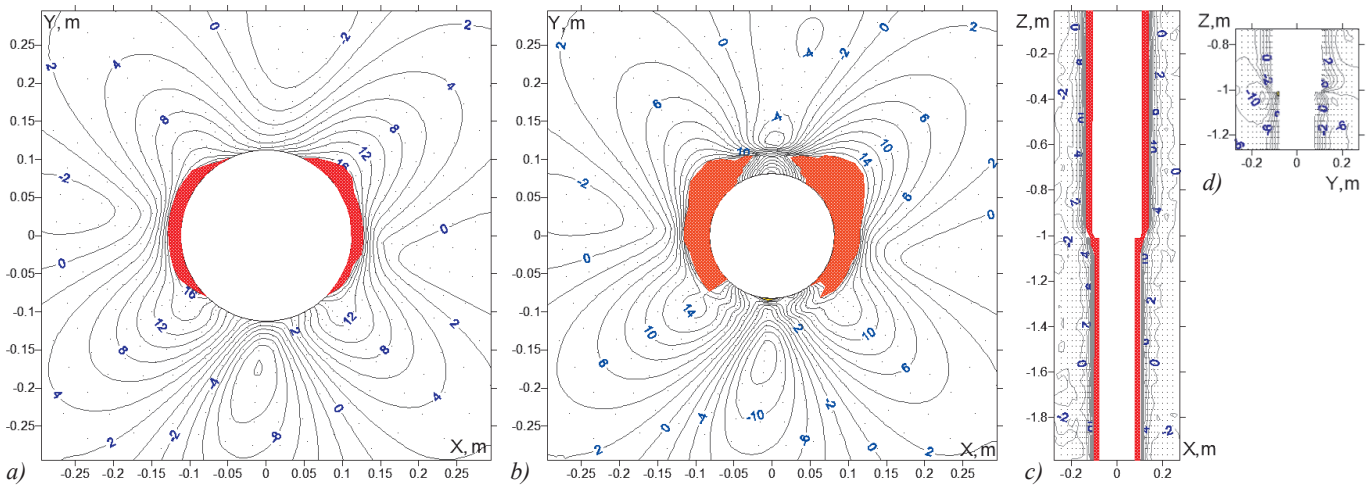

Fig. 14. Changing the shapes of destructed areas at reduced pressure drop (dP = 20 atm) in a 220/160 mm junction. The section XY is related to h = 0.99 m (a) and h = 1.01 m (b). Increased breakouts can be seen in the XZ section (c). A hydrofracture can be seen in the enlarged YZ section (d).

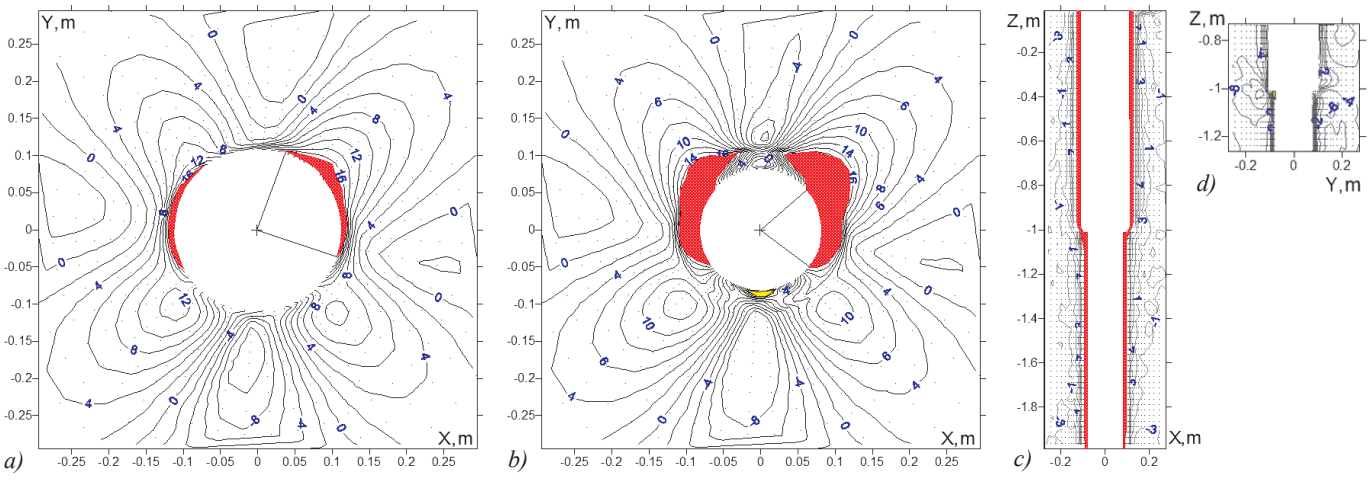

Fig. 15. Shapes of destructed areas around a 220/160 mm junction at dP = 50 atm. The section XY is related to h = 0.99 m (a) and h = 1.01 m (b). The XZ and enlarged YZ sections can be seen in (c) and (d) respectively.

Increasing dP up to 50 atm in the 220/160 mm junction causes the angular size of breakouts to reduce, so it becomes smaller than 90° (Figure 15 a, b). Taking into account that the hydrofracture is still localized in the juncture's shoulder (Figure 15, c, d), we can conclude that the junction is stable.

Analogous behavior can be observed in the 160/120 mm juncture, which makes core drilling at dP = 50 atm in such a borehole stable as well.

If in the 220/160 mm juncture, dP increases up to 60 atm, it produces a tensile failure across the juncture's shoulder in the YZ section (Figure 16, a) that elongates downward into the bottom hole. The dispositions of the shear and fracturing areas in a plane perpendicular to the well's axis can be seen in Figure 16 (b).

If in the 160/120 mm junction the pressure drop increases up to 60 atm, it leads to formation of two azimuthal hydrofractures on the opposite walls of the well, and the length of these fractures is bigger than the length of such fractures in the 220/160 mm juncture, which can be seen in Figure 17 (a). The shapes of breakouts as well as the positions of the hydrofractures are demonstrated in Figure 17 (b).

In general, since in the considered junctions the hydrofractures are nonlocal, core drilling at dP = 60 atm should be considered as unstable.

Further increase of the pressure drop in both inclined junctions 220/160 mm and 160/120 mm provokes further hydrofractures propagation downward the bottom hole and upward the main borehole, which is demonstrated in the section YZ presented in Figure 18. It is apparent that core drilling at dP = 70 atm is dangerous.

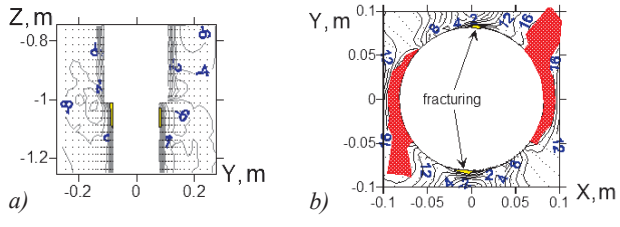

Fig. 16. Shapes of destructed areas around a 220/160 mm junction at dP = 60 atm. In the YZ section, a hydrofracture propagates from the junction's shoulder downward the bottom hole. Another hydrofracture can be seen on the opposite wall. The XY section is related to h = 1.05 m (b). The shear failure areas keep reducing.

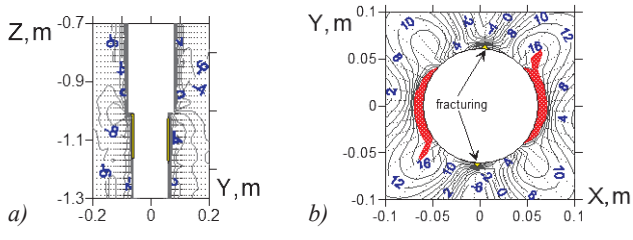

Fig. 17. Areas of destruction around a 160/120 mm junction at dp = 60 atm. The YZ section (a) shows the extension of the hydrofractures. The disposition of the fractures and breakouts relative to the well's contour can be seen in the XY section (b) at h = 1.1 m.

Discussion

The junction stability results were obtained with the help of the vertical transversely isotropic poroelastic model with mudcake buildup taken into account. Due to the slight variation in the elastic parameters reconstructed from the core compression tests the question of the applicability of the isotropic approach to describe the behavior of the formation arises. The modeling of the stress state for isotropic medium was carried out for the vertical and inclined wellbore junction taken into account mudcake growth. Comparison of the results with a vertical transversely isotropic case showed that the difference in the equivalent stress in the area of different diameters wells joining is 6–15%. Due to the fact that experimental data on core deformation are more accurately described by a model with anisotropic properties this system of

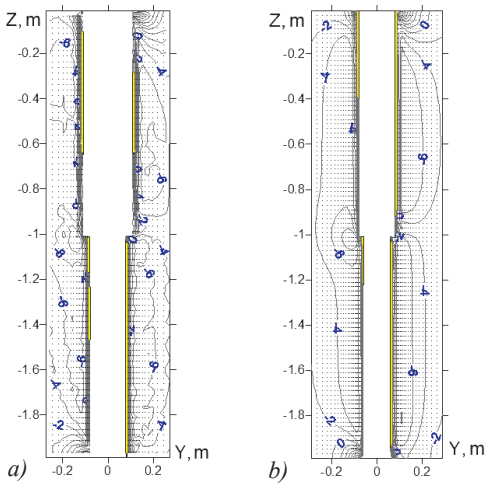

Fig. 18. Propagation of hydrofractures at dP = 70 atm around 220/160 mm (a) and 160/120 mm (b) junctions in the YZ section

equations for a poroelastic medium was chosen for numerical calculations.

The important result is that there are no fundamental differences between the 220/160 mm and 160/120 mm junctions when it comes to the type and character of the failure zones that occurs around the joints at changing pressure drop. It other words, the main conclusions concerning stability while core drilling can be generalized for both cases.

Applying the "standard" pressure drop of 40 atm while core drilling with a bit of smaller diameter has proved to be insufficient due to the size of breakouts indicates the juncture's wall instability. The drilling becomes safe if the applied pressure drop increases by 10 atm.

In the anisotropic sandstones of the Surgut Dome, it is better to perform core sampling in either vertical or sub-vertical wells. The modeling has demonstrated that the vertical junction is more stable because it is not prone to hydrofracturing even when the pressure drop reaches 70 atm.

In inclines wells, whose inclination angle is 60° and higher, drilling with a bit of smaller diameter should be performed keeping within quite a narrow window of mud pressure. So, while drilling at pressure drop equals to 50 atm is enough to stabilize an inclined juncture, its decrease by 10 atm leads to critical shear failure while the increase by 10 atm – to hydraulic fracturing of the borehole's walls.

The area most prone to fracturing is the juncture's shoulder where the main and bottom holes diameters meet. It can be assumed that, in reality, rock chipping smooths this area forming a seamless transition area between the holes.

It is also should be noticed that the bottom hole of the vertical junctures is more resistant to a reduced pressure drop because the destructions are initiated in the main wellbore and then spread downward to the bottom one. On the contrary, in the inclined junctures at increased pressure drop, tensile fracture first occur in the bottom hole to spread into the main borehole making the last more stable to an increased dP.

Conclusions

The performed 3D poroelastic modeling of vertical and inclined 220/160 mm and 160/120 mm well junctions in the anisotropic sandstone of the Akh Formation productive pay for a pressure-drop range from 1 to 70 atm has demonstrated that:

- The shape and character of fracturing around the junctions are qualitatively similar for the diameters ratios in question at equal pressure drops;
- The vertical junctions are more stable if compared to the inclined ones since their formation excludes hydraulic fracturing;
- While core sampling from vertical wells, one should maintain a pressure drop above 55 atm down the hole to guarantee the well's stability;
- In the vertical junctions, the bottom hole is more stable to pressure drop reduction;
- In order to provide stability of the inclined junctions, a pressure drop should be maintained at 50 atm ±10%. Reducing the pressure drop leads to the critical spalling of the walls, and increasing – to propagation of a tensile fracture along the borehole's surface;
- Increasing the pressure drop in the inclined junctions initiates hydraulic fracturing in the bottom hole, while the main borehole preserves its stability.

References

Ashikhmin S.G., Kashnikov Yu.A., Shustov D.V., Kukhtinskii A.E. (2018). Influence of elastic and strength anisotropy on the stability of inclined borehole. *Neftyanoe khozyaistvo = Oil Industry*, 2, pp. 54–57. https://doi.org/10.24887/0028-2448-2018-2-54-57

Bocharov O.B., Seryakov A.V. (2016). Modeling uncharacteristic destruction of productive sandstone layers during drilling. *Fizicheskaya Mezomekhanika*, 19(6), pp. 86–93.

Cheng A. H.-D. (1997). Material Coefficients of Anisotropic Poroelasticity. *Int. J. Rock Mech. Min. Sci*., 34(2), pp. 199–205. https://doi.org/10.1016/S0148-9062(96)00055-1

Cui L., Cheng A.H-D., and Y. Abousleiman (1997). Poroelastic Solution for an Inclined Borehole. *J. of App. Mechanics ASME*, 64(1), pp. 32–38. https://doi.org/10.1115/1.2787291

Fadeev A.B. (1987). Finite element method in geomechanics. Moscow: Nedra, 221 p.

Geniev G.A., Kurbatov A.S, Samedov F.A. (1993). Issues of strength and ductility of anisotropic materials. Moscow: Interbuk, 187 p.

Grogulenko V.V. (2017). Modeling the application of loads on metal-polymer coiled tubing pipes for the oil and gas industry. *Naukovedenie*, 9(1).

Liu C., and Y. Abousleiman (2018). Multiporosity/Multipermeability Inclined-Wellbore Solutions With Mudcake Effects. *SPE Journal*, 23(5), pp. 1723–1747. https://doi.org/10.2118/191135-PA

Mohamad-Hussein A. and J. Heiland (2018). 3D finite element modelling of multilateral junction wellbore stability. *J. Pet. Sci*., 15, pp. 801–814. https://doi.org/10.1007/s12182-018-0251-0

Podberezhny M., Polushkin S. and Makarov A. (2017). Novel Approach for Evaluation of Petrpphysical Parameters from Time-Lapse Induction Logging-While-Drilling Measurements in Deviated and Horizontal Wells. *Proc. SPE Conf*. Moscow. https://doi.org/10.2118/187911-RU

Rudyak V.Ya., Seryakov A.V., Manakov A.V. (2013). Joint modeling of geomechanics and filtration processes in the near-wellbore zone while drilling. *Proc. Conf.: Geodynamics and the stress state of the Earth's interior.* Novosibirsk: IGD SO RAN, v.1, pp. 383–388.

Seryakov A.V, Podberezhnyi M.Yu., Bocharov O.B. (2018). Formation anisotropy as a key factor in well stability in the West Salym field. *Proceedings of the 8th International Geological and Geophysical Conference EAGE: Innovations in Geoscience – Time for Breakthrough*. St. Petersburg.

Zoback M.D. (2010). Reservoir Geomechanics. Cambridge University Press, 449 p.

About the Authors

Alexander V. Seryakov – Researcher, Cand. Sci. (Engineering)

Novosibirsk Technology Center, Baker Hughes

4A Kutateladze st., Novosibirsk, 630090, Russian Federation

Maxim Yu. Podberezhny – Head of Petrophysics Department, Cand. Sci. (Physics and Mathematics)

Gazpromneft-GEO

22A Sinopskaya emb., St. Petersburg, 191167, Russian Federation

Oleg B. Bocharov – Deputy Director for HP, , Cand. Sci. (Physics and Mathematics)

Novosibirsk Technology Center, Baker Hughes

4A Kutateladze st., Novosibirsk, 630090, Russian Federation

Marat A. Azamatov – Head of Short-Term Development Planning, Master of Physics

Salym Petroleum Development N.V.

31 Novinsky boul., Moscow, 123242, Russian Federation

Manuscript received 19 December 2019;
Accepted 4 June 2020; Published 30 September 2020